

RECENT ADVANCES IN MODELING OF PEROVSKITE SOLAR CELLS USING SCAPS-1D: EFFECT OF ABSORBER AND ETM THICKNESS[†]

 Eli Danladi^{a,*}, Douglas Saviour Dogo^b, Samuel Udeh Michael^c, Felix Omachoko Uloko^d, Abdul Azeez Omeiza Salawu^e

^aDepartment of Physics, Federal University of Health Sciences, Otuokpo, Benue State, Nigeria

^bDepartment of Physics, Federal College of Education (Technical) Omoku, Rivers State, Nigeria

^cDepartment of Physics, Nigerian Defence Academy, Kaduna, Nigeria

^dDepartment of Physics, Federal University, Lokoja, Kogi State, Nigeria

^eDepartment of Computer Science, Nile University of Nigeria

*Corresponding Author: danladielibako@gmail.com, tel. +2348063307256

Received August 28, 2021; revised November 15, 2021; accepted November 16, 2021

With the massive breakthrough recorded in the power conversion efficiency (PCE) of perovskite solar cells (PSCs) from 3.8 % to > 25 %, PSCs have attracted considerable attention in both the academia and industries. However, some challenges remain as barrier in realizing its deployment. To develop a highly efficient PSCs as well as environmentally benign device, simulation and optimization of such devices is desirable. Its impractical as well as wastage of time and money to design a solar cell without simulation works. It minimizes not only the risk, time and money rather analyzes layers' properties and role to optimize the solar cell to best performance. Numerical modeling to describe PV thin layer devices is a convenient tool to better understand the basic factors limiting the electrical parameters of the solar cells and to increase their performance. In this review article, we focused on the recent advances in modelling and optimization of PSCs using SCAPS-1D with emphasis on absorber and electron transport medium (ETM) thickness.

Keywords: perovskite solar cells, absorber, electron transport medium, SCAPS

PACS: 41.20.Cv; 61.43.Bn; 68.55.ag; 89.30.Cc; 68.55.jd; 73.25.+i; 72.80.Tm; 74.62.Dh; 78.20.Bh;

INTRODUCTION

Perovskite solar cells, as a promising class of device belonging to the third-generation solar cell, have gained global interest due to their simple processing procedure and low cost [1]. Hybrid perovskite are defined on the basis of AMX_3 crystal structure, where A is an organic cation, for example, methylammonium or formamidinium, M is a metal and X is a halogen atom. The combination of amazing advantages, such as excellent tolerance for perovskite crystal defects, availability for superior light absorption efficiency, efficient carrier mobility and enough carrier diffusion lifetimes promote this as a candidate for outstanding solar cell photovoltaic performance [1-7]. In general, the competitiveness of solar cells is evaluated by efficiency, cost and lifetime, where scalability is closely related to cost and lifetime has much to do with stability [8]. Achieving a balance of efficiency, cost and lifetime is the key to promote the commercialization of PSCs to grab a share of the energy market. Therefore, several research efforts are addressing these issues that are important for commercialization. A few unprecedented achievements have been made that are highly beneficial for the large-scale commercial application of PSCs in the future [9-11].

In PSCs, the absorber layer, which is used for harvesting photon energy is crucial. It is the central part of PSCs mostly determines the overall device performance. Many studies have demonstrated that the PCE of PSCs is generally dependent on thickness of the perovskite absorber [12-15]. Thickness of electron transport layers are also crucial for better efficiencies [13-17].

In this article, the progress of PSC development is reviewed, concentrating on the perovskite and electron transport functional layer, and valuable insights are provided. Other sections discussed the effect of thickness of absorber and ETM on the photovoltaic properties of perovskite solar devices.

OPERATION PRINCIPLE OF A PEROVSKITE SOLAR CELL

The working principle of the PSC is described in Figure 1. Photons from the light source reach the perovskite layer via glass (TCO) and transparent electrodes. In the active perovskite layer, photons are absorbed and excitons are excited when the incident energy of the photon is greater than that of the perovskite material. The exciton is split into electrons and holes by an internal potential created by the difference in the work function between the transparent electrode and metallic electrode. Electrons are transferred to Electron Transporting Layer (ETL) and holes are transferred to Hole Transporting Layer (HTL). From there, the electrons move to the transparent electrode and the holes move to the metal electrode. Next, the electrons travel through a network that connects the two electrodes, and the traveling electrons produce an electric current. For the PSC to function properly, the energy levels in each layer must be carefully configured to prevent the recombination of excited charge carriers. However, since they are also energy conservers, they always follow the path of least resistance [18]. The correct structure of the layers prevents recombination within the cell as the charge carriers pass through different paths. This is achieved by creating an ETL Lowest Unoccupied Molecular Orbital

[†] Cite as: E. Danladi, D.S. Dogo, S.U. Michael, F.O. Uloko, and A.O. Salawu, East. Eur. J. Phys. 4, 5 (2021), <https://doi.org/10.26565/2312-4334-2021-4-01>
© E. Danladi, D.S. Dogo, S.M. Udeh, F.O. Uloko, 2021

(LUMO) lower than the perovskite LUMO layer. This creates a more attractive way for electrons to move. The same applies to HTL Highest Occupied Molecular Orbital (HOMO). HTL HOMO must be higher than the perovskite HOMO layer. This creates a more attractive path for holes to go. This is the same for each layer in the cell. Each layer has a higher HOMO or lower LUMO for the normal operation of the charge carrier transport chain, as shown in Figure 1.

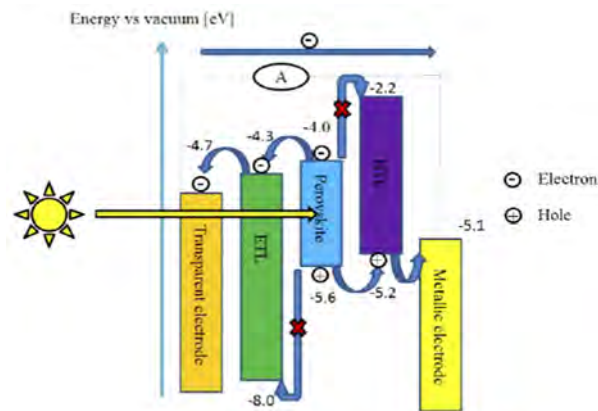


Figure 1. Schematic of the operational principle of perovskite solar cell [18]

Device Structure

The architecture of the device is a fundamental tool in evaluating the PCE of PSCs. Perovskite solar cells are generally classified into regular (n-i-p) and inverted (p-i-n) structures depending on which transport (electron/hole) material is present on the exterior portion of the cell/encountered by incident light first [19]. These two designs are subdivided into two classes: mesoscopic and planar structures. The mesoscopic structure is made of a mesoporous layer whereas the planar structure consists of all planar layers. Some designs do not involve electron and hole-transporting layers. Summarily, about six types of perovskite solar cell architectures have been designed and tested by several researchers thus far: the mesoscopic n-i-p configuration, the planar n-i-p configuration, the planar p-i-n configuration, the mesoscopic p-i-n configuration, the ETL-free configuration, and the HTL-free configuration [19].

Regular n-i-p structure

The conventional n-i-p mesoscopic structure was the first structure developed and tested, it involves the replacement of light-harvesting dye with lead halide perovskite absorber in a traditional dye-sensitized solar cell (DSSC)-type architecture [20]. The interest was sold to many researchers when the initial structure (Fig. 2a) were built by replacing the liquid electrolyte with a solid-state hole-conductor [21]. This breakthrough in the architecture has created a pathway for photovoltaic scholars and consequently led to the development of other PSC device structures (Fig. 2b-d). The planar architecture is an evolution of the mesoscopic structure, where the perovskite light-harvesting layer is sandwiched between the ETM and HTM. The absence of a mesoporous metal oxide layer leads to an overall simpler structure.

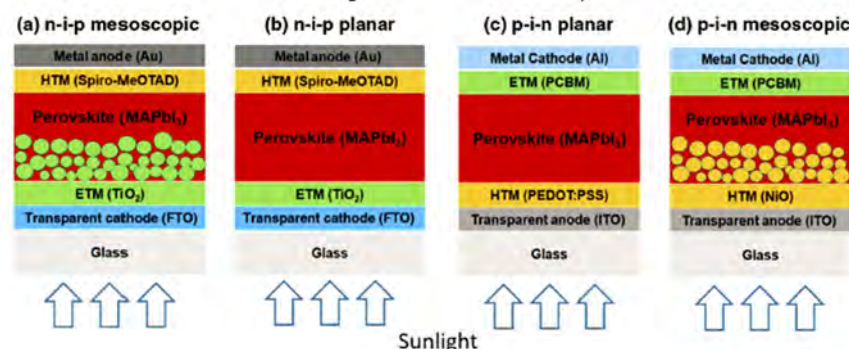


Figure 2. Schematic showing the layered structure of four typical perovskite solar cells (a) n-i-p mesoscopic, (b) n-i-p planar, (c) p-i-n planar, and (d) p-i-n mesoscopic [19,22]

Inverted p-i-n structure

The p-i-n perovskite solar cell design was first derived from the organic solar cell reported [23]. In the case of the p-i-n planar perovskite structure, the hole transport layer (HTL) is first deposited followed by the electron transport layer (ETL). It was discovered that perovskite absorbers can simultaneously absorb photon energy and transport the holes themselves [19,24], and this led to the development of planar hetero-junction PSC with an inverted structural design [25]. With this record breakthrough, the inverted p-i-n structure has expanded the horizon of photovoltaics and permits mesoscopic p-i-n device architecture [19]. The device structure of the inverted p-i-n planar and mesoscopic PSC is shown in Fig. 2c, d.

Effect of thickness of absorber

The absorber layer of the perovskite solar cell plays an essential role in device performance and outcome. Therefore, the proper choice of thickness of the absorber can considerably affect the performance and results of a solar cells. Thickness of absorber is an essential factor to be considered in a solar cell device as such a comprehensive understanding of its role in solar cell is necessary. Eli et al. [26] investigated the effect of thickness of absorber with TiO_2 and inorganic cuprous oxide (Cu_2O) as ETM and HTM ranging from 0.2 to 0.9 μm . The influence of thickness of absorber on the solar cell parameters (V_{OC} , J_{SC} , FF and PCE) were evaluated. PCE is lower when thickness of the absorber is 0.2 μm which can be attributed to the poor light absorption by the layer. However an increased in PCE was observed as a result of increase of the absorber layer thickness from 0.20 to 0.40 μm , thereafter, it starts decreasing. For thickness beyond 0.4 μm , the collection of photo generated carriers decreased because of charge recombination [26]. The best performing device was observed with thickness of 0.40 μm which gave optimized parameters (PCE of 12.83%. J_{sc} of 21.43 mA/cm^2 , V_{oc} of 0.86V, and FF of 69.51%). The JV curve and variation of the thickness with parameters is as shown in Fig. 3 [26]. Their studies demonstrate that careful selection of absorber thickness results to good performing PSCs. Similar studies with variation in absorber thickness from 0.1 to 1.0 μm was carried out [27]. Short circuit current (J_{sc}) increases from 12.33 to 22.36 mA/cm^2 with thickness increase from 0.1 to 0.6 μm which is attributed to the increase in carrier generation and dissociation, then starts decreasing from 0.7 to 1.0 μm . It was also observed that the Fill Factor (FF) decreases with thickness increase in the perovskite layer. The PCE increase with increase in layer thickness from 0.1 to 0.4 μm was due to the production of new charge carriers. However, PCE decreases from thickness of 0.5 μm to 1.0 μm (Table 1) due to lesser electron and hole pairs extraction rate that leads to recombination process [28].

Table 1. J-V characteristic parameters with the variation of thickness of absorber

Parameters T (μm)	J_{sc} (mA/cm^2)	V_{oc} (V)	FF	PCE (%)
0.1	12.34	0.77	79.12	7.48
0.2	17.85	0.82	77.16	11.30
0.3	20.42	0.84	74.32	12.78
0.4	21.63	0.86	71.39	13.21
0.5	22.17	0.86	68.54	13.13
0.6	22.36	0.87	65.36	12.85
0.7	22.36	0.88	63.59	12.46
0.8	22.24	0.88	61.39	12.02
0.9	22.06	0.88	59.50	11.60
1.0	21.85	0.89	57.73	11.18

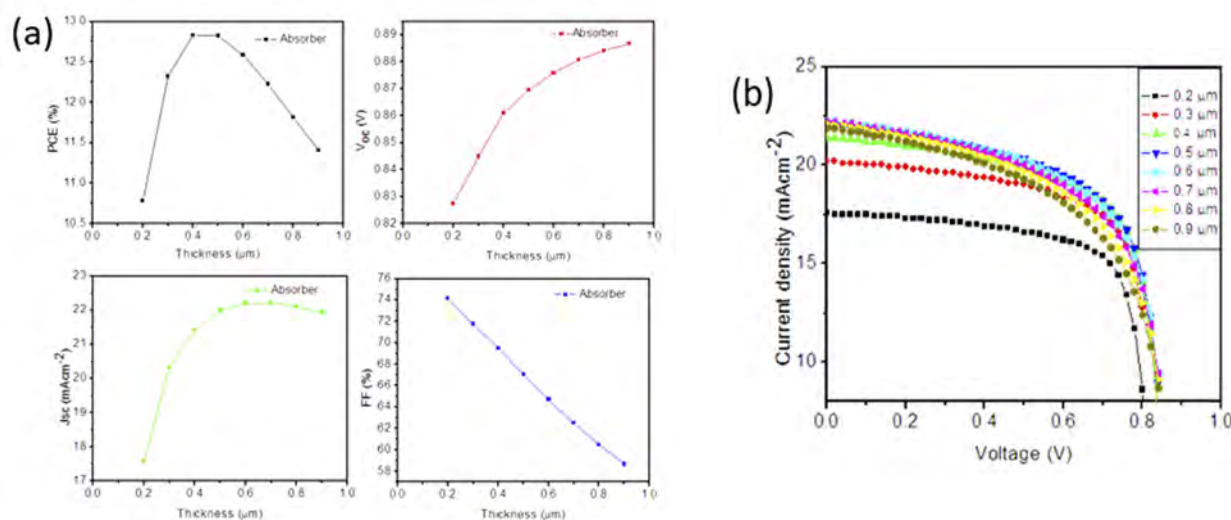


Figure 3. (a) Variation in performance parameters of PSC with thickness of Absorber, (b) J–V curves of PSC with different values of Absorber thickness [26].

Another study that show the beneficial role of absorber thickness on solar cell performance (V_{OC} , J_{SC} , FF and PCE) is described in Figure 4 (a). The J-V and QE of the varied absorber thickness is shown in Figure 4 (b) and (c).

Figure 4 (c) exhibits the spectral response of the PSCs as a function of wavelength with varied $\text{CH}_3\text{NH}_3\text{PbI}_3$ layer thickness within range of 300 nm to 900 nm. The QE first increases rapidly with the $\text{CH}_3\text{NH}_3\text{PbI}_3$ thickness increasing from $0.1 \mu\text{m}$ to $0.4 \mu\text{m}$, and the QE increase slightly after the thickness is greater than $0.4 \mu\text{m}$, which shows that $0.4 \mu\text{m}$ thickness of $\text{CH}_3\text{NH}_3\text{PbI}_3$ layer can absorb most of the incident photons and the part beyond $0.4 \mu\text{m}$ can only contribute little to the PSC performance. Therefore, the optimized perovskite absorber layer thickness is around $0.4 \mu\text{m}$ which gives V_{OC} of 0.86 V, J_{SC} of 21.63 mAcm^{-2} , FF of 71.31 % and PCE of 13.21 %.

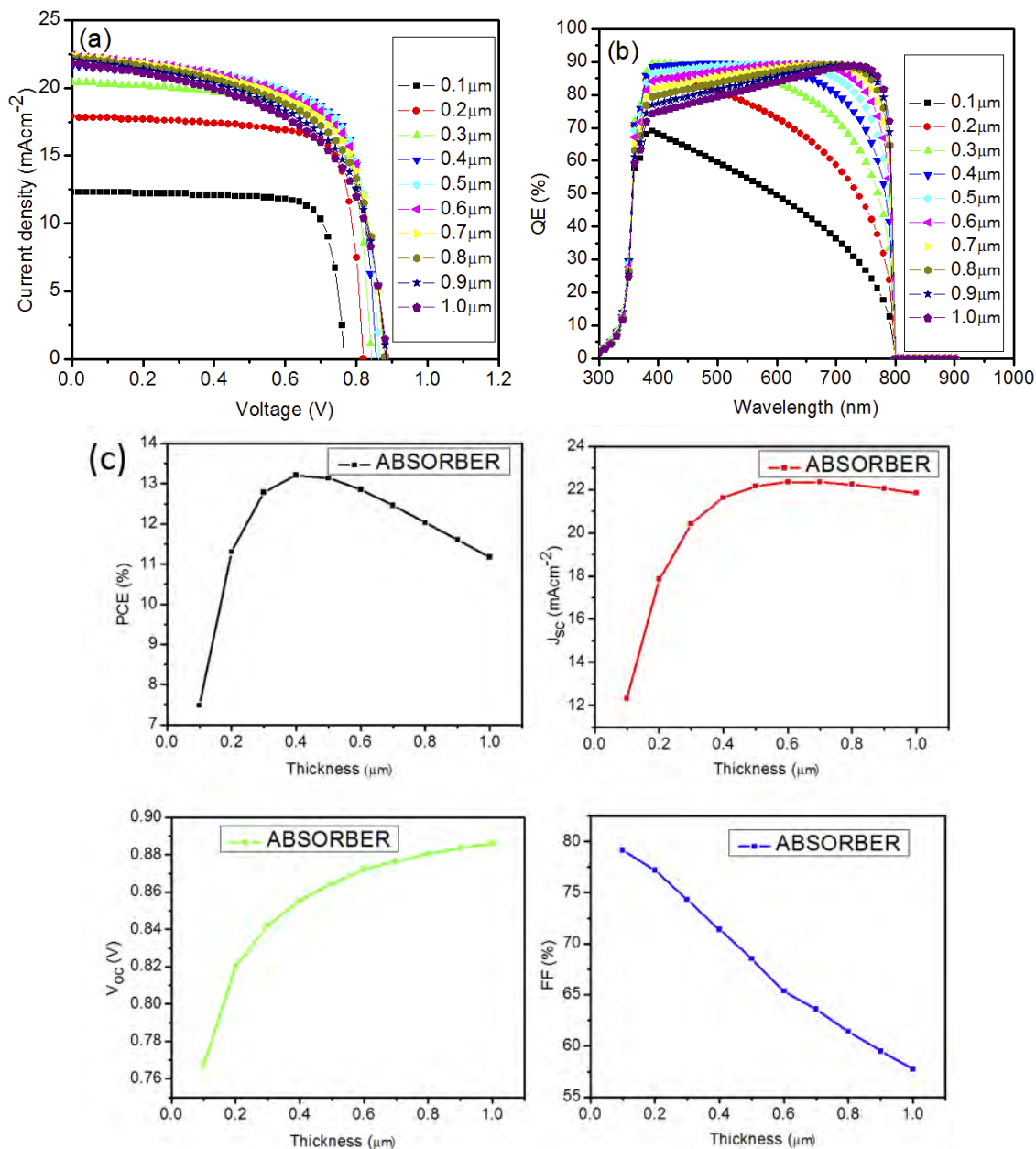


Figure 4 (a) J–V curves of PSC with different values of thickness of absorber layer, (b) QE with different values of thickness of absorber layer, (c) Variation in performance parameters of PSC with thickness of absorber layer [27].

The effect of thickness on PV and Quantum efficiencies of PSCs with ZnSe as ETL and Cu_2O as ETL was also studied [29]. The simulation was carried out in the range of 0.03 to 1.5 μm while other parameters are kept constant. Table 2 [29] shows the effect with respect to varied absorber thickness.

Similarly, Muhammad et al. [30] systematically investigated the effect of absorber thickness in lead free PSC with copper iodide as HTM and found out that the thickness of absorber affects the performance of perovskite solar cells as shown in Fig. 5 [30].

Hussain and co researchers [31] also studied the effect of absorber layer thickness on PCE of lead free hybrid double PSCs with spiro-meOtd as HTM. In their study, absorber layer thickness was varied from 100 nm to 1000 nm, and the effect was observed on the output parameters while all other parameters are set constant. The deviation in device outcomes with the thickness of the active layer is depicted in Fig 6 and Table 3 [31]. The simulation results show that with the

increase in thickness of the active layer, short-circuit current J_{sc} increases and approaches to the optimum value of $\sim 39 \text{ mAcm}^{-2}$.

The influence of thickness of absorber on the performance parameters was also studied by Haider et al. [32]. They made use of lead based perovskite absorber with inorganic HTM and ETM as transport medium for holes and electrons. The variation of the absorber thickness was from 100 to 1000 nm. PCE is lower when thickness of the layer is too small due to the poor light absorption, which means that small thicknesses are not favorable for good light harvesting in PSC. PCE of PSCs increases with the increase of the thickness of the absorber before reaching a constant value at 600 nm. For absorber thicker than 600 nm, the collection of photo generated carriers decreased because of charge recombination, which also shows that thicker absorber layer act as center for recombination of charge carriers. Fig. 7(b) indicates that QE increases with the increase of absorber thickness up to 300 nm thickness. After 300 nm thickness, no significant increase in QE is observed. Carrier diffusion length is the crucial factor in designing perovskite solar cell structure [32-34] which depends on the absorber thickness (Fig. 7c).

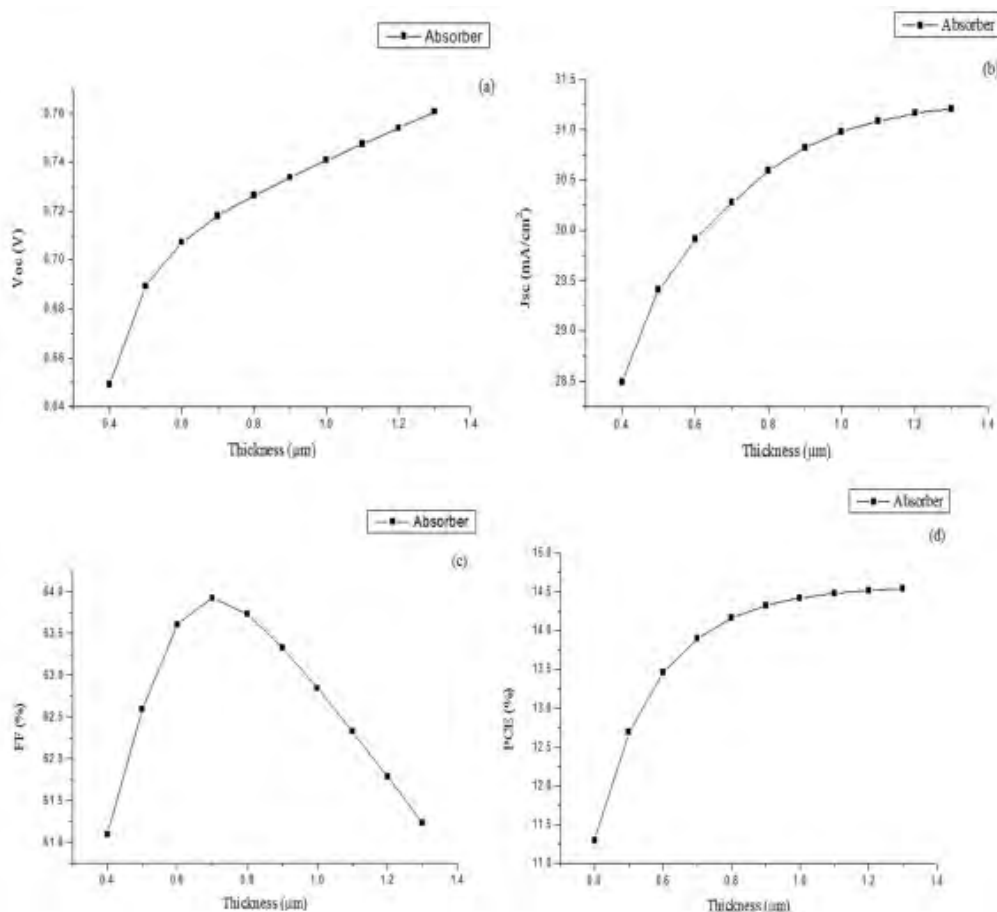


Figure 5. Variation of Absorber thickness with photovoltaic performance [30]

Table 2. Dependence of solar cell performance on absorber layer [29].

Absorber thickness (μm)	J_{sc} (mA/cm^2)	V_{oc} (V)	FF (%)	PCE (%)
0.03	8.87	0.76	74.99	5.08
0.09	16.76	0.80	74.53	10.11
0.2	24.73	0.84	72.11	15.15
0.5	31.32	0.89	68.29	19.08
0.7	32.44	0.89	67.77	19.65
1.9	32.91	0.89	67.44	19.82
1.2	33.16	0.89	67.08	19.81
1.5	33.23	0.88	66.77	19.71

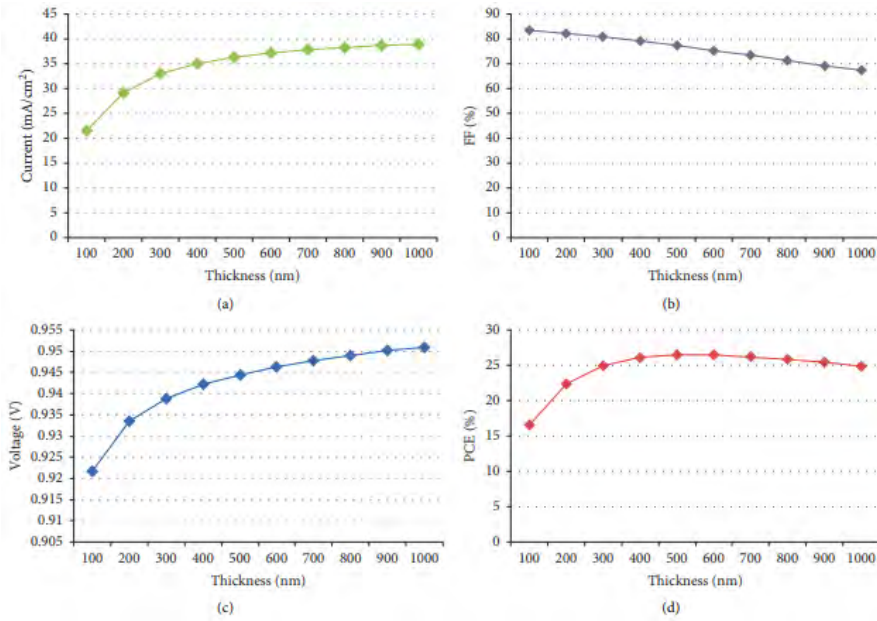


Figure 6. (a) Short-circuit current density as a function of absorber thickness. (b) Fill factor as a function of absorber thickness. (c) Open circuit voltage as a function of absorber thickness. (d) PCE as a function of absorber thickness [31].

Table 3. Device Performance at a different absorber layer thickness [31]

Thickness (nm)	V_{oc} (volt)	FF (%)	J_{sc} (mA/cm ²)	PCE (%)
100	0.9216	83.60	21.56	16.61
200	0.9335	82.24	29.18	22.40
300	0.9388	80.73	32.95	24.98
400	0.9421	79.08	35.03	26.10
500	0.9445	77.28	36.31	26.50
600	0.9463	75.36	37.16	26.50
700	0.9478	73.39	37.77	26.28
800	0.9491	71.38	38.23	25.90
900	0.9501	69.34	38.59	25.42
1000	0.9510	67.28	38.88	24.88

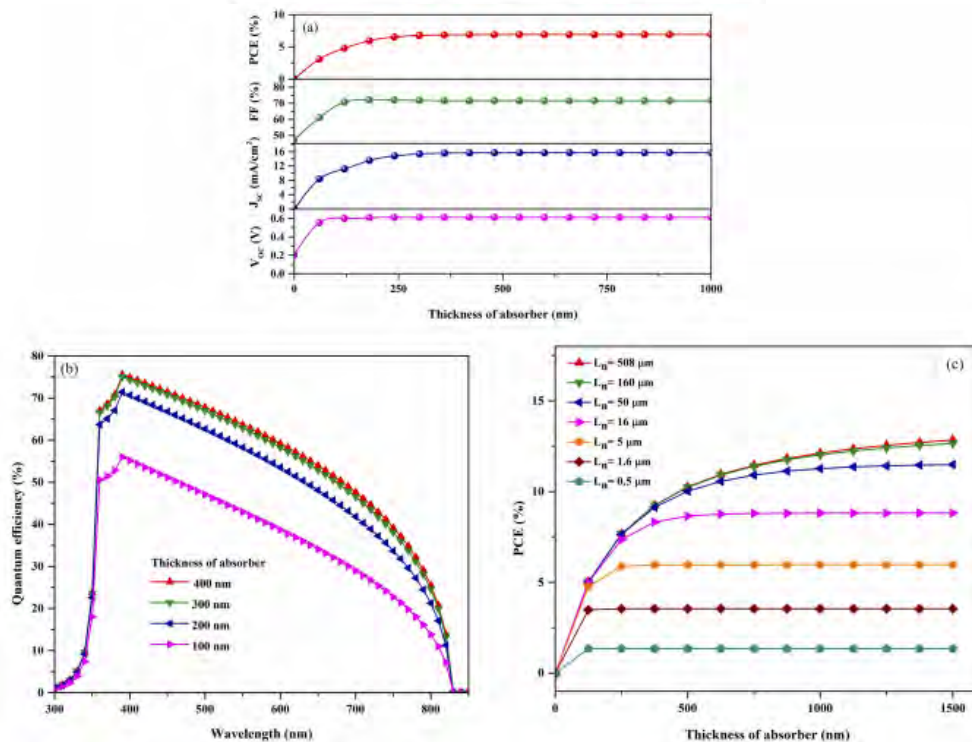


Figure 7. Variation in (a) performance parameters and (b) quantum efficiency of PSC with different thickness of absorber layer (c) variation in PCE with various diffusion lengths and thickness of absorber layer [32].

Also, a simulation was done by changing the absorber thickness from 0.1 μm to 2 μm and maintaining all the other device parameters constant [35]. As shown, J_{sc} increases with the increasing thickness (Fig. 8a), which is attributed to the generation of more electron-hole pairs in the perovskite leading to an efficiency enhancement. The highest efficiency of 21.42% is obtained at an optimum thickness of 0.5 μm . However, a decrease in efficiency in the thicker absorber layer is due to a reduced electric field, which affects the charge carriers' recombination behaviour within the absorber [36]. This statement has been confirmed in the recombination profile with an increasing recombination at the perovskite/Spiro-meOtdad junction with a thickness (Fig. 8c). FF is inversely proportional to the perovskite thickness due to an increased series resistance and an internal power dissipation in a thicker absorber layer (Fig. 8b). The decrease in V_{oc} with the thickness (Fig. 8b) is attributed to the increment in the dark saturation current, which increases the recombination of the charge carriers. That can be explained by the dependency of open-circuit voltage on the photo-generated current and dark saturation current, which is written as [37]:

$$v_{oc} = \frac{kT}{q} \ln \left[\frac{J_{sc}}{J_0} + 1 \right], \quad (1)$$

where kT/q is the thermal voltage, J_{sc} is the photo-generated current density, and J_0 is the saturation current density.

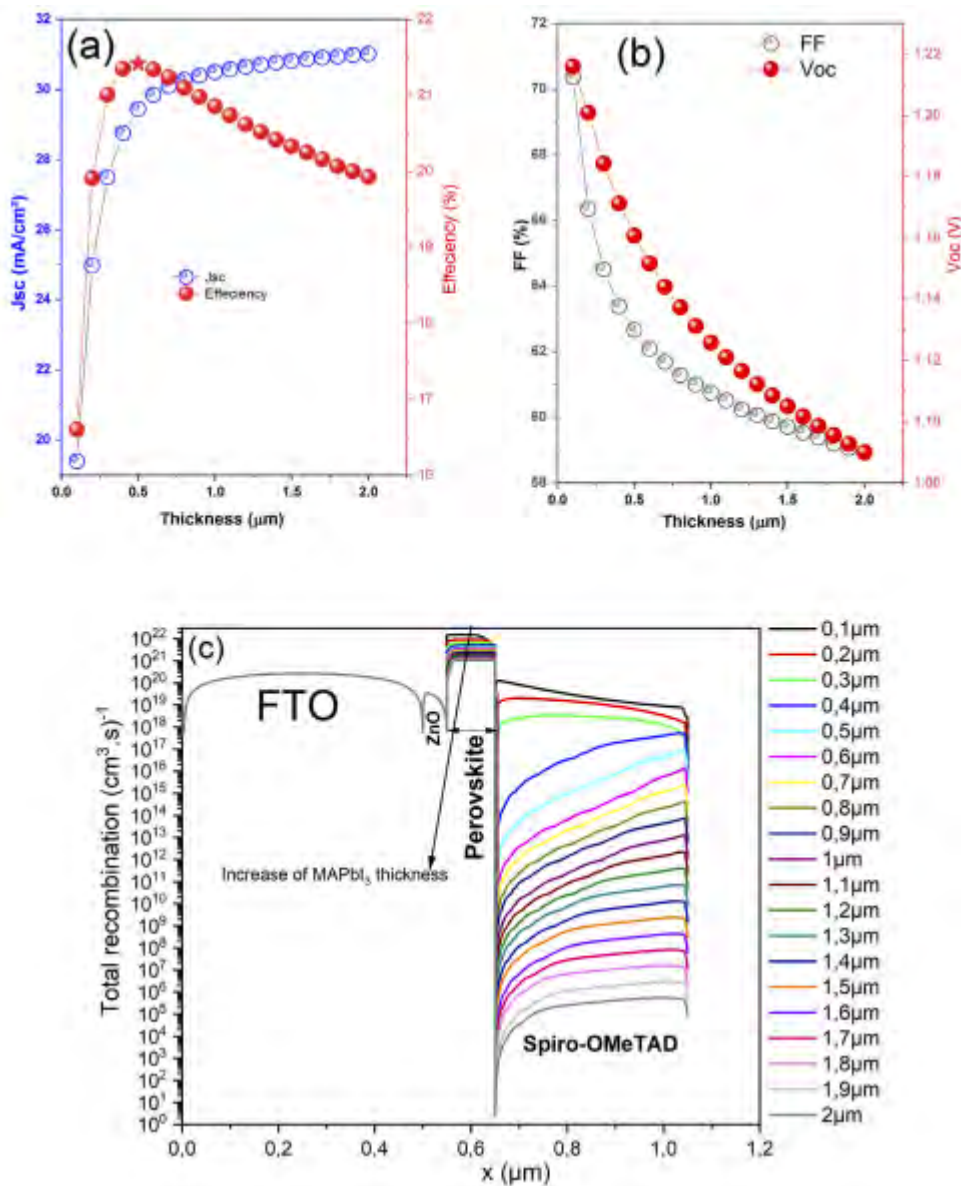


Figure 8. The variation of (a) J_{sc} , PCE, (b) FF, V_{oc} as well as (c) total recombination profile versus the thickness of MAPbI_3 [35].

Soucase et al. [38], also studied the effect of thickness of absorber from 50 nm to 700 nm under 1 Sun (AM1.5G) illumination without considering interface trap density of states but consideration of inputs value of band tail density of states, and Gaussian acceptor/donor states of MAPbI_3 to be $10 \times 10^{14} \text{ eV}^{-1} \text{ cm}^{-3}$ and $10 \times 10^{14} \text{ cm}^{-3}$ respectively. The short

circuit current and PCE both are found to be increased sharply with increase in thickness up to 500 nm (Fig. 9a) [38]. After this, increment is very slow and reaches to almost optimal efficiency 25.22%, V_{OC} 1.2 V, J_{SC} 25.49 mA/cm² and FF 82.56% at 700 nm [38]. The quantum efficiency curves as a function of wavelength of incident light for different thickness of the absorber (Fig. 9b) also verifies the above mentioned upshot.

Several other authors have also studied the effect of perovskite thickness [39-47] using SCAPS and their studies show that, poor film quality can affect the coverage of perovskite on ETL. If the quality of film is poor, then defect density increases and recombination rate of carriers becomes dominant in absorber layer which determine the V_{oc} of the solar cell [32]. Therefore, substantive studies should be carried out to determine the best thickness for optimum PSC performance.

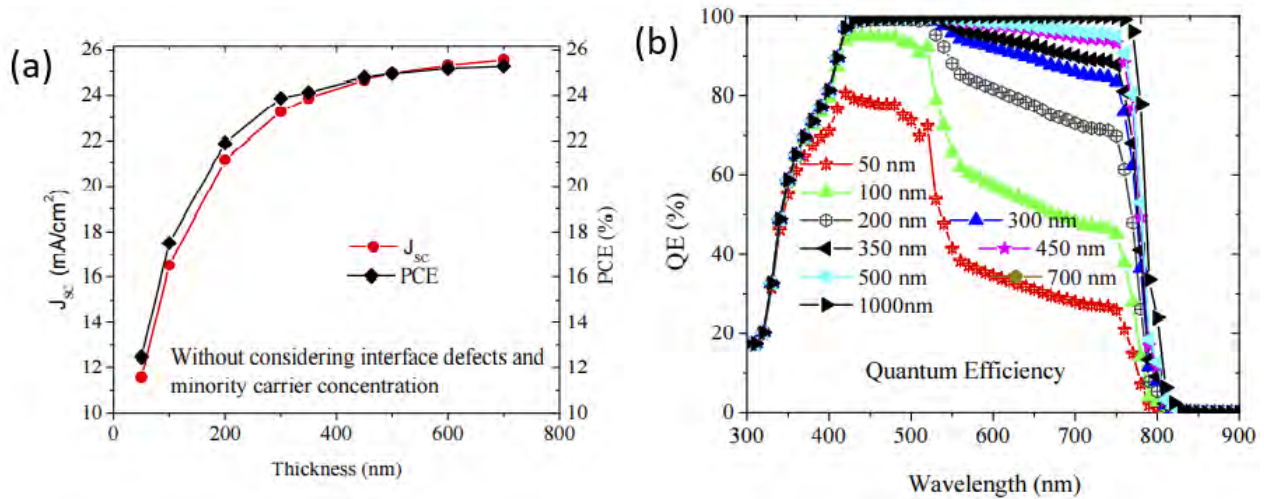


Figure 9. (a) J_{sc} and PCE vs Thickness, (b) Variation of quantum efficiency with thickness of absorber [38].

Effect of ETL thickness

The thickness properties of the ETM affect the conduction of charge carrier between the front and back contacts [48]. Efficient collection of the charge carriers depends on work function of the front contact material and rear metallization [60]. And most importantly, the selection of the appropriate ETM plays a significant role on the design and implementation of high efficiency perovskite solar cell as the energy band alignment between absorber and ETM layer is a crucial factor for the efficiency improvement of PSCs [48,49].

Soucase et al. [38] studied the effect of thickness of two ETMs (TiO_2 and ZnO) with spiro-meOtatd as HTM. In both cases V_{OC} , J_{SC} and PCE gradually decreases due to fractional absorption of incident light by the ETMs layer, the bulk recombination and surface recombination at the interface and change in series resistance [38, 49]. The thickness of ETMs was varied from 50 nm to 450 nm to make the practical devices. Results from the studies showed that TiO_2 is more sensitive than that of ZnO due to its high absorption coefficient and reflectance and less transmittance than ZnO [38]. This shows that, increase in thickness of ETM lessen the performance of solar cells due to increase in partial absorption of photons and resistance of the device. Also, study was carried out by simulation by the same group of researchers with practically viable thickness of TiO_2 – ETM (Fig. 10).

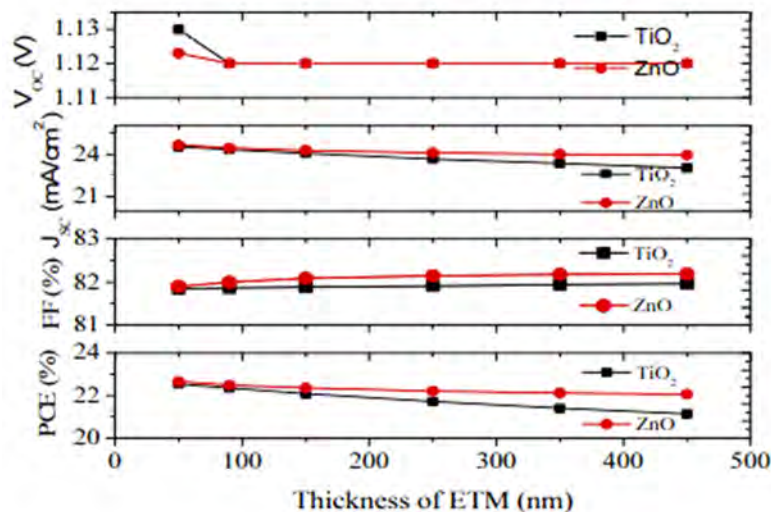


Figure 10. Variation of PV cells parameters with thickness of ETMs [38].

In a HTM free PSCs, where the absorber is simultaneously absorbing light and transporting holes, the thickness of ETM was varied from 0.02 to 0.10 μm . The results show that both the PCE, J_{sc} , V_{oc} and FF decrease with the thickness of ETM (Fig 11, Table 4) [27]. Fig. 11b, shows the QE of the PSCs as a function of wavelength in the range of 300-900 nm with varied ETM layer thickness. The studies show that QE maximum value was obtained in the wavelength range of 380–570 nm and gradually decreases at longer wavelengths until 800 nm, which corresponds to its absorption spectrum.

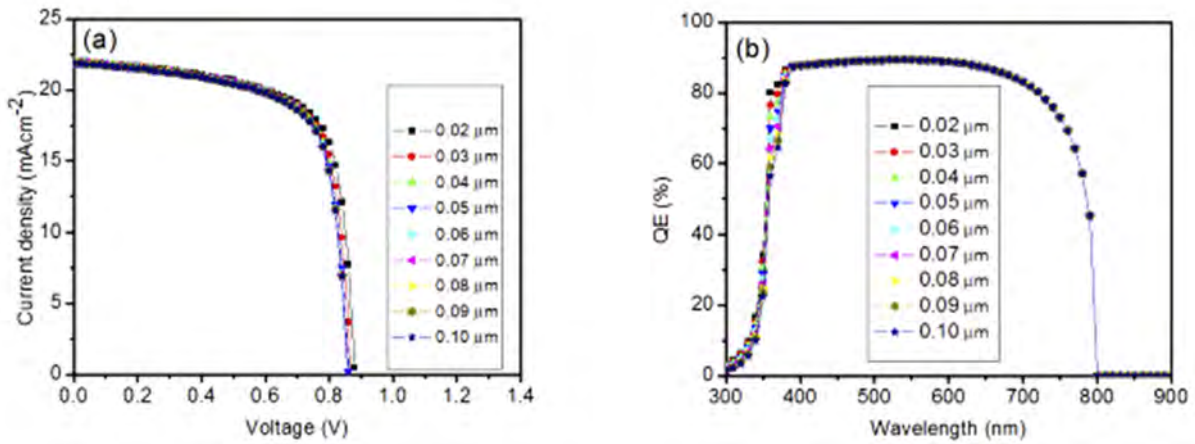


Figure 11. (a) J-V curves of PSC with different values of thickness of ETM, (b) QE with different values of thickness of ETM [27].

Table 4. J-V characteristic parameters with the variation of thickness of ETM [27]

Parameters T (μm)	J_{sc} (mAcm^{-2})	V_{oc} (V)	FF	PCE (%)
0.02	22.05	0.88	70.17	13.63
0.03	22.01	0.87	70.11	13.40
0.04	21.98	0.86	69.96	13.28
0.05	21.96	0.86	69.94	13.22
0.06	21.94	0.86	69.91	13.18
0.07	21.93	0.86	69.91	13.17
0.08	21.92	0.86	69.91	13.15
0.09	21.90	0.86	69.91	13.15
0.10	21.89	0.86	69.92	13.14

Effect of ETL layer thickness in PSC with ZnSe and Cu_2O as ETM and HTM was explored in the range of 0.005 to 0.080 μm . The results after the simulation show that when there is an increase in the thickness of electron transporting material it results in decrease in J_{sc} , FF and PCE of the device while V_{oc} decreases but remain invariable from 0.89 V at the thickness of 0.010 μm (Table 3).

Table 2. Dependence of solar cell performance of the thickness of ZnSe (ETL) [29].

ZnSe thickness (μm)	J_{sc} (mA/cm^2)	V_{oc} (V)	FF (%)	PCE (%)
0.0050	33.13	0.90	68.16	20.44
0.0100	32.91	0.89	67.76	20.03
0.0150	32.81	0.89	67.75	19.90
0.0300	32.63	0.89	67.75	19.77
0.0350	32.58	0.89	67.75	19.74
0.0450	32.49	0.89	67.76	19.68
0.0500	32.44	0.89	67.77	19.65
0.0800	32.18	0.89	67.79	19.50

Their study signifies that when the material is thicker, it provides a longer diffusion path for the electron to reach the electrode which limit (solar cell parameters) the charge collection efficiency and transmitting of incident photon

decreases with increasing thickness. The optimized device performance was obtained, when the thickness of ETL was $0.005\mu\text{m}$ with J_{SC} of $33.13\text{mA}/\text{cm}^2$, V_{OC} of 0.90V , FF of 68.16% and high PCE of 20.44% [29]. Also, different ETMs (TiO_2 , ZnO and SnO_2) were simulated in PSCs with thickness variation from 90 nm to 200 nm . It was observed that with the increase of thickness $>90\text{ nm}$, a decrease in V_{oc} , J_{sc} and thus PCE in case of TiO_2 and ZnO , was observed (Fig. 12) [50], while in the case of SnO_2 , there was no noticeable change in its value. It was found that TiO_2 was more affected than ZnO and SnO_2 due to its lower transmittance in $300\text{-}400\text{ nm}$ range and possesses low electron mobility, thus reduction in J_{sc} value occurs as a function of increased ETM thickness, which can be ascribed to the partial absorption of incident light by thicker TiO_2 and ZnO layer.

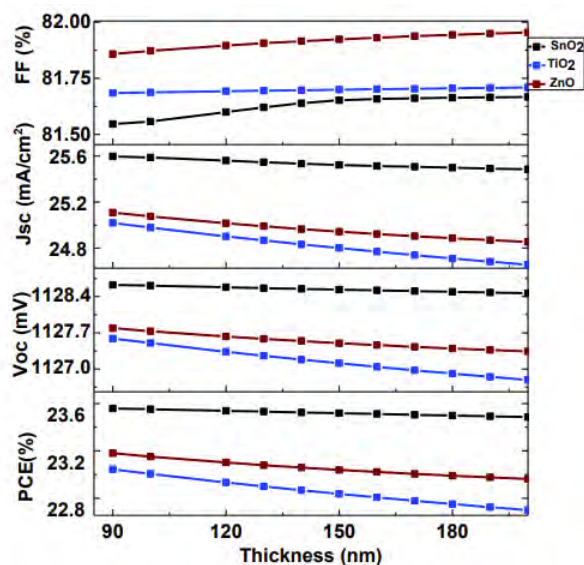


Figure 12. Effect of different ETM thickness on photovoltaic parameters of MAPbI_3 based planar perovskite solar cells using Spiro-OMeTAD as HTM [50].

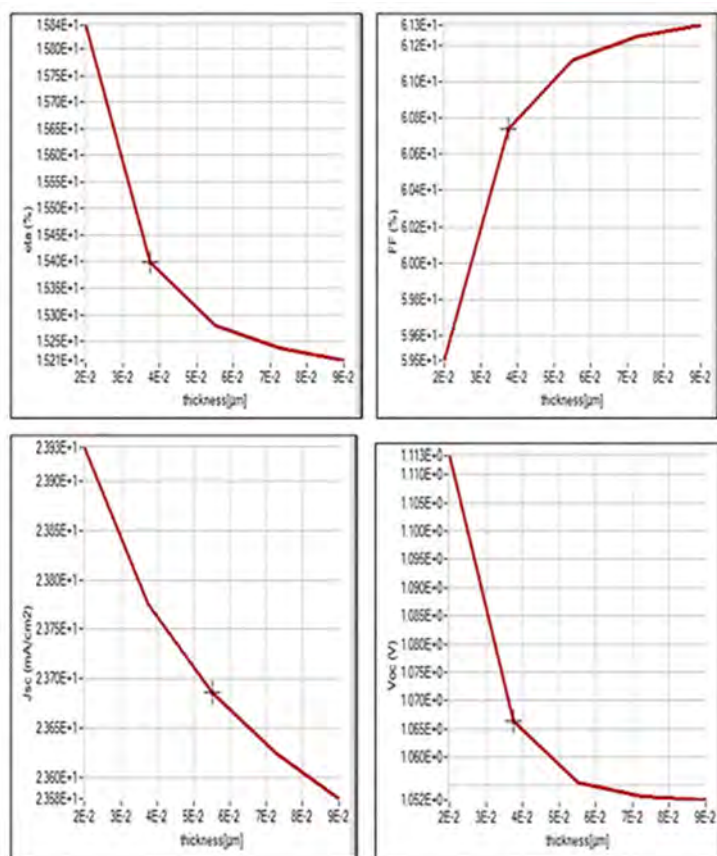


Figure 13. Variation of efficiency, fillfactor, J_{sc} , and V_{oc} with respect to thickness of ETM layer [58].

Hence it decreases the rate of charge generation and collection and consequently short circuit current (J_{sc}) decreases [50-53]. However, in case of SnO_2 , due to its high transparency, active layer absorption is less affected and J_{sc} did not decrease significantly up to a certain thickness of 150 nm thus rate of charge generation rate increases as compared to the recombination. Moreover, due to high carrier mobility and high carrier concentration of SnO_2 , the series resistance decreases with the thickness due to increase in conductivity and thus fill factor also increases up to certain thickness of 150 nm and beyond this insignificant changes occurs. Some notable achievements in PSCs using SCAPS has been reported too [30,54-57]. Also, a studies with variation of thickness of ZnO as ETM was conducted by Aseena et al. [58]. The study explains the effect of ETM layer thickness on the PSC parameters. The results showed that the efficiency decreases slightly from 15.84% to 15.24% as thickness is increased from 20 nm to 90 nm (Fig. 13). This confirms that the electron transport layer does not have much effect on the electrical parameters of the perovskite solar cell [58]. An ETM free perovskite planar structure solar cells was designed and implemented [59]. This is explained on the basis of the fact that perovskite material itself could help the generation of charge carriers by photon

excitation and ETM layer is just a charge transport layer. Even in the absence of the ETM, the transparent conducting oxide (Fluorine doped tin oxide) layer will act as charge transport layer without affecting the efficiency [58,59]. But however, fill factor could be improved by the application of an optimal layer of ETM [60]. But the gradual increase in ETM layer thickness can also reduce the performance of PSC by increasing photon absorption and resistance of the cell [38].

Sultana et al. [49] also shows how the thickness of ETM affects photovoltaic parameters (Fig. 14). It was shown that, the variation of thickness towards getting optimum performance influence the performance of PSCs. From the three different ETMs (TiO_2 , ZnO and SnO_2) used, 400 nm thicknesses are taken for both MAPbI_3 (absorber) and spiro-OMeTAD (HTM) layer.

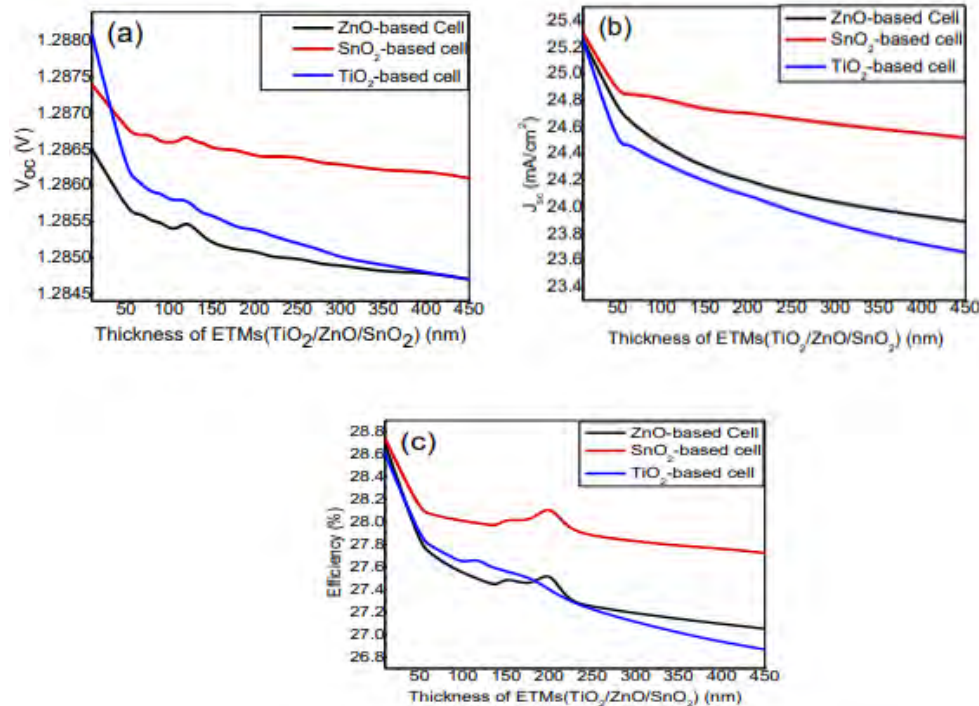


Figure 14. Photovoltaic performances of three models by varying thickness of ETM (a) Open circuit voltage; (b) Short circuit current density; (c) Photovoltaic conversion efficiency [49].

Their ETM layer thickness was varied from 10 nm to 450 nm and a gradual decrease of V_{oc} , J_{sc} and PCE was observed. The overall performance of solar cell with SnO_2 as ETM is higher than other two models for the entire thickness range. At lower thickness (10 nm to 180 nm), TiO_2 -based model gives better performance than ZnO based cell, but for thickness higher than 250 nm ZnO-base model shows better efficiency than TiO_2 [49]. The observation showed that TiO_2 is more responsive to sunlight than that of the other two electron collecting materials as it has higher absorption coefficient and reflectance and less transmittance [48, 49]. It was shown from their work that the increase in thickness of ETM result to poor performance of the solar cells. This can be ascribed to fractional absorption of incident light by ETMs and variation in series resistance of the device with increasing thickness of ETM layer [26,49]. Efficiencies of 27.6 %, 27.5% and 28.02% are found for TiO_2 , ZnO and SnO_2 -base cell respectively at 90 nm thickness of electron collecting material [48].

CONCLUSION

We have summarized and discussed recent developments in simulation of perovskite solar cells using solar capacitance simulator software with emphasis on thickness of absorber and ETM and its influence with variation on the photovoltaic performance of perovskite solar cells. The review shows that the proper choice of thickness of the absorber can considerably affect the performance and results of solar cells. Also, selection of the appropriate ETM and its thicknesses plays a significant role on the design and implementation of high efficiency perovskite solar cells as the energy band alignment between absorber and ETM layer is a crucial factor for the efficiency improvement of PSCs.

ORCID IDs

©Eli Danladi, <https://orcid.org/0000-0001-5109-4690>

REFERENCES

- [1] D. Eli, M.Y. Onimisi, S. Garba, and J. Tasiu, SN Applied Science, **2**, 1769 (2020), <https://doi.org/10.1007/s42452-020-03597-y>
- [2] D. Eli, M.Y. Onimisi, S. Garba, P.M. Gyuk, T. Jamila, and H.P. Boduku, IOP Conference Series, Material Science and Engineering, **805**, 012005 (2020), <https://doi.org/10.1088/1757-899X/805/1/012005>
- [3] M.U. Samuel, M.Y. Onimisi, J.A. Owolabi, D. Eli, and E.O. Mary, The Proceedings of the Nigerian Academy of Science, **13(1)**, 148 (2020), <https://nasjournal.org.ng/index.php/pnas/article/view/320/162>

- [4] J. Jin, J. Li, Q. Tai, Y. Chen, D.D. Mishra, W. Deng, J. Xin, S. Guo, B. Xiao, and X. Wang, *Journal of Power Sources*, **482**, 228953 (2021), <https://doi.org/10.1016/j.jpowsour.2020.228953>
- [5] M. Minbashi, A. Ghobadi, M.H. Ehsani, H. Rezagholipour Dizaji, and N. Memarian, *Solar Energy*, **176**, 520 (2018), <http://dx.doi.org/10.1016/j.solener.2018.10.058>
- [6] K. Kumari, A. Jana, A. Dey, T. Chakrabarti, and S.K. Sarkar, *Optical Materials*, **111**, 110574 (2021), <https://doi.org/10.1016/j.optmat.2020.110574>
- [7] P.K. Patel, *Scientific Reports*, **11**, 3082 (2021), <https://doi.org/10.1038/s41598-021-82817-w>
- [8] X. Dai, K. Xu, and F. Wei Beilstein, *Journal of Nanotechnology*, **11**, 51 (2020), <https://doi.org/10.3762/bjnano.11.5>
- [9] X. Zhu, Z. Xu, S. Zuo, J. Feng, Z. Wang, X. Zhang, K. Zhao, J. Zhang, H. Liu, S. Priya, S. F. Liu, and D. Yang, *Energy & Environmental Science*, **11**, 3349 (2018), <https://doi.org/10.1039/C8EE02284D>
- [10] F. Di Giacomo, S. Shanmugam, H. Flederius, B.J. Bruijnaers, W.J.H. Verhees, M.S. Dorenkamper, S.C. Veenstra, W. Qiu, R. Gehlhaar, T. Merckx, T. Aernouts, R. Andriessen, and Y. Galagan, *Solar Energy Materials and Solar Cells*, **181**, 53 (2018), <https://doi.org/10.1016/j.solmat.2017.11.010>
- [11] Y. Zong, Z. Zhou, M. Chen, N.P. Padture, and Y. Zhou, *Advanced Energy Materials*, **8**, 1800997 (2018), <https://doi.org/10.1002/aenm.201800997>
- [12] I.J. Ogundana, and S.Y. Foo, *Journal of Solar Energy*, **2017**, Article ID 8549847, <https://doi.org/10.1155/2017/8549847>
- [13] F. Izadi, A. Ghobadi, A. Gharaati, M. Minbashi, and A. Hajjiah, *Optik*, **227**, 166061 (2021), <https://doi.org/10.1016/j.ijleo.2020.166061>
- [14] C.W. Chang, Z.W. Kwang, T.Y. Hsieh, T.C. Wei, and S.Y. Lu, *Electrochimica Acta*, **292**, 399 (2018), <https://doi.org/10.1016/j.electacta.2018.09.161>
- [15] M. Rai, L.H. Wong, and L. Etgar, *Journal of Physical Chemistry Letters*, **11**(19), 8189 (2020), <https://doi.org/10.1021/acs.jpcclett.0c02363>
- [16] A. Ślawek, Z. Starowicz, and M. Lipin´ski, *Materials*, **14**, 3295 (2021), <https://doi.org/10.3390/ma14123295>
- [17] A. Kumar, S.K. Ojha, N. Vyas, and A.K. Ojha, *ACS Omega*, **6**(10), 7086 (2021), <https://doi.org/10.1021/acsomega.1c00062>
- [18] J. Stenberg, Master's Thesis, Umea University, (2017).
- [19] I. Hussain, H.P. Tran, J. Jaksik, J. Moore, N. Islam, and M.J. Uddin, *Emergent materials*, **1**, 133 (2018), <https://doi.org/10.1007/s42247-018-0013-1>
- [20] A. Kojima, K. Teshima, Y. Shirai, and T. Miyasaka, *Journal of American Chemical Society*, **131**, 6050 (2009), <https://doi.org/10.1021/ja809598r>
- [21] H.S. Kim, C.R. Lee, J.H. Im, K.B. Lee, T. Moehl, A. Marchioro, S.J. Moon, R. Humphry-Baker, J.H. Yum, J.E. Moser, M. Grätzel, and N.G. Park, *Scientific Reports*, **2**, 591 (2012), <https://doi.org/10.1038/srep00591>
- [22] Z. Song, S.C. Wathage, A.B. Phillips, M.J. Heben, *Journal of Photonics for Energy*, **6**, 022001 (2016), <https://doi.org/10.1117/1.JPE.6.022001>
- [23] L. Meng, J. You, T.-F. Guo, and Y. Yang, *Accounts of Chemical Research*, **49**(1), 155 (2016), <https://doi.org/10.1021/acs.accounts.5b00404>
- [24] J.Y. Jeng, Y.F. Chiang, M.H. Lee, S.R. Peng, T.F. Guo, P. Chen, and T.C. Wen, *Advanced Materials*, **25**, 3727 (2013), <https://doi.org/10.1002/adma.201301327>
- [25] L. Hu, K. Sun, M. Wang, W. Chen, B. Yang, J. Fu, Z. Xiong, X. Li, X. Tang, Z. Zang, S. Zhang, L. Sun, and M. Li, *ACS Applied Materials & Interfaces*, **9**(50), 43902 (2017), <https://doi.org/10.1021/acsami.7b14592>
- [26] D. Eli, M.Y. Onimisi, S. Garba, R.U. Ugbe, J.A. Owolabi, O.O. Ige, G.J. Ibeh, and A.O. Muhammed, *Journal of the Nigerian Society of Physical Sciences*, **1**, 72 (2019), <https://doi.org/10.46481/jnsps.2019.13>
- [27] E. Danladi, A. Shuaibu, M. S. Ahmad, and J. Tasiu, *East European Journal of Physics*, **2021**(2), 135 (2021), <https://doi.org/10.26565/2312-4334-2021-2-11>
- [28] U. Mandadapu, S.V. Vedanayakam, and K. Thyagarajan, *International Journal of Engineering Science and Invention*, **2**, 40 (2017).
- [29] J.A. Owolabi, M.Y. Onimisi, J.A. Ukwenya, A.B. Bature, U.R. Ushiekpan, *American Journal of Physics and Applications*, **8**(1), 8, (2020), <http://dx.doi.org/10.11648/j.ajpa.20200801.12>
- [30] A.O. Muhammed, E. Danladi, H.P. Boduku, J. Tasiu, M.S. Ahmad, and N. Usman, *East European Journal of Physics*, **2021**(2), 146 (2021), <https://doi.org/10.26565/2312-4334-2021-2-12>
- [31] S.S. Hussain, S. Riaz, G.A. Nowsherwan, K. Jahangir, A. Raza, M.J. Iqbal, I. Sadiq, S.M. Hussain, and S. Naseem, *Journal of Renewable Energy*, **2021**, Article ID 6668687 (2021), <https://doi.org/10.1155/2021/6668687>
- [32] S.Z. Haider, H. Anwar, and M. Wang, *Semiconductor Science and Technology*, **33**, 035001 (2018), <https://orcid.org/0000-0002-0473-850X>
- [33] M.M. Tavakoli, L. Gu, Y. Gao, C. Reckmeier, J. He, A.L. Rogach, Y. Yao, and Z. Fan, *Scientific Reports*, **5**, 14083 (2015), <https://doi.org/10.1038/srep14083>
- [34] A.A. Paraecattil, J. De Jonghe-Risse, V. Pranculis, J. Teuscher, and J.E. Moser, *Journal of Physical Chemistry C*, **120**, 19595 (2016), <https://doi.org/10.1021/acs.jpcc.6b08022>
- [35] T. Ouslimane, L. Et-taya, L. Elmaimouni, and A. Benami, *Heliyon*, **7**, e06379 (2021), <https://doi.org/10.1016/j.heliyon.2021.e06379>
- [36] J.P. Correa-Baena, M. Anaya, G. Lozano, W. Tress, K. Domanski, M. Saliba, T. Matsui, T.J. Jacobsson, M.E. Calvo, A. Abate, M. Grätzel, H. Míguez, and A. Hagfeldt, *Advanced Materials*, **28**, 5031 (2016), <https://doi.org/10.1002/adma.201600624>
- [37] P. Singh, and N.M. Ravindra, *Solar Energy Materials and Solar Cells*, **101**, 36 (2012), <https://doi.org/10.1016/j.solmat.2012.02.019>
- [38] B.M. Soucase, I.G. Pradas, and K.R. Adhikari, in: *Perovskite Materials - Synthesis, Characterisation, Properties, and Applications*, (49659), 445 (2016), <https://doi.org/10.5772/61751>
- [39] M. Kaifi, and S.K. Gupta, *International Journal of Engineering Research and Technology*, **12**(10), 1778 (2019).
- [40] G.A. Nowsherwan, K. Jahangir, Y. Usman, M.W. Saleem, M. Khalid, *Scholars Bulletin*, **7**(7), 171 (2021), <https://doi.org/10.36348/sb.2021.v07i07.004>

- [41] U.C. Obi, M.Sc. thesis, department of material science and engineering, African university of science and technology, Abuja, Nigeria (2019).
- [42] M.T. Islam, M.R. Jani, S. Rahman, K.M. Shorowordi, S.S. Nishat, D. Hodges, S. Banerjee, H. Efstathiadis, J. Carbonara, and S. Ahmed, *SN Applied Sciences*, **3**, 504 (2021), <https://doi.org/10.1007/s42452-021-04487-7>
- [43] M.I. Samiul, K. Sobayel, A. Al-Kahtani, M.A. Islam, G. Muhammad, N. Amin, M. Shahiduzzaman, and M. Akhtaruzzaman, *Nanomaterials*, **11**, 1218 (2021), <https://doi.org/10.3390/nano11051218>
- [44] U. Mandadapu, S.V. Vedanayakam, and K. Thyagarajan, *Indian Journal of Science and Technology*, **10**(11), 1 (2017).
- [45] U. Mandadapu, S.V. Vedanayakam, K.K. Thyagarajan, and B.J. Babu, *International Journal of Simulation and Process Modelling*, **13**(3), 221 (2018), <https://dx.doi.org/10.1504/IJSPM.2018.093097>
- [46] M.R. Ahmadian-Yazdi, F. Zabihi, M. Habibi, and M. Eslamian, *Nanoscale Research Letters*, **11**, 408 (2016), <https://doi.org/10.1186/s11671-016-1601-8>
- [47] J. Barbé, M.L. Tietze, M. Neophytou, B. Murali, E. Alarousu, A. El Labban, M. Abulikemu et al, *ACS Appl. Mater. Interfaces*, **9**, 11828 (2017), <https://doi.org/10.1021/acsami.6b13675>
- [48] K.R. Adhikari, S. Gurung, B.K. Bhattarai, and B.M. Soucase, *Physica Status Solidi C*, **13**(1), 13 (2016), <https://doi.org/10.1002/pssc.201510078>
- [49] N.A. Sultana, M.O. Islam, M. Hossain, and Z.H. Mahmood, *Dhaka University Journal of Science*, **66**(2), 109 (2018), <http://dx.doi.org/10.3329/dujs.v66i2.54553>
- [50] Y. Raoui, H. Ez-Zahraouy, N. Tahiri, O. El Bounagui, S. Ahmad, and S. Kazim, *Solar Energy*, **193**, 948 (2019), <https://doi.org/10.1016/j.solener.2019.10.009>
- [51] A. Singla, R. Pandey, R. Sharma, J. Madan, K. Singh, V.K. Yadav, and R. Chaujar, in: *2018 IEEE Electron Devices Kolkata Conference (EDKCON)*, pp. 278-282 (2018).
- [52] T. Kirchartz, T. Agostinelli, M. Campoy-Quiles, W. Gong, and J. Nelson, *The Journal of Physical Chemistry Letters*, **3**, 3470 (2012), <https://doi.org/10.1021/jz301639y>
- [53] I. Alam, and M.A. Ashraf, *Energy Sources, Part A: Recovery, Utilization, and Environmental Effects*, (2020).
- [54] S. Yasin, T. Al Zoubi, and M. Moustafa, *Optik*, **229**, 166258 (2021), <https://doi.org/10.1016/j.ijleo.2021.166258>
- [55] F.A. Afak, M. Nouredine, S.A. Meftah, *Solar Energy*, **181**, 372 (2019), <https://doi.org/10.1016/j.solener.2019.02.017>
- [56] M. Kumar A. Raj, A. Kumar, and A. Anshul, *Materials Today Communications*, **26**, 101851 (2021), <https://doi.org/10.1016/j.mtcomm.2020.101851>
- [57] N. Singh, A. Agarwal, and M. Agarwal, *AIP Conference Proceedings*, **2265**, 030672 (2020), <https://doi.org/10.1063/5.0016929>
- [58] S. Aseena, N. Abraham, and V.S. Babu, *Materials Today: Proceedings*, **43**(6), 3432 (2021), <https://doi.org/10.1016/j.matpr.2020.09.077>
- [59] L. Huang, X. Sun, C. Li, R. Xu, J. Xu, Y. Du, Y. Wu, J. Ni, H. Cai, et al, *Solar Energy Materials and Solar Cells*, **157**, 1038 (2016), <https://doi.org/10.1016/j.solmat.2016.08.025>
- [60] A. Hima, N. Lakhdar, B. Benhaoua, A. Saadoun, I. Kemerchou, and F. Rogti, *Superlattices and Microstructures*, **129**, 240 (2019), <https://doi.org/10.1016/j.spmi.2019.04.007>

ОСНОВНІ УСПЕХИ В МОДЕЛЮВАННЯ ПЕРОВСКІТОВИХ СОНЯЧНИХ ЕЛЕМЕНТІВ ВИКОРИСТАННЯ SCAPS-1D: ВПЛИВ ПОГЛИНАЧА ТА ТОВЩИНИ ЕТМ

Елі Данладі^a, Дуглас Сейвіор Дого^b, Семюел Уде Міхаел^c,
Фелікс Омачко Улоко^d, Абдул Азіз Омейза Салаву^e

^aКафедра фізики, Федеральний університет медико-санітарних наук, Отужно, штат Бенуе, Нігерія

^bКафедра фізики, Федеральний освітній (технічний) коледж Омоку, штат Ріверс, Нігерія

^cКафедра фізики, Нігерійська академія оборони, Кадуна, Нігерія

^dКафедра фізики, Федеральний університет, Локоджа, штат Когі, Нігерія

^eКафедра комп'ютерних наук Нігерійського університету Нілу

З великим проривом, зафіксованим у ефективності перетворення енергії (PCE) перовскітних сонячних елементів (PSC) з 3,8 % до > 25 %, PSC привернули значну увагу як у наукових колах, так і в промисловості. Однак деякі проблеми залишаються перешкодою для реалізації їх розгортання. Для розробки високоефективних PSC, а також екологічно безпечних пристроїв, бажано моделювати та оптимізувати такі пристрої. Проектувати сонячну батарею без імітаційних робіт непрактично, а також є витратним час та коштів. Проектування мінімізує не тільки ризик, час і гроші, а аналізує властивості та роль шарів для оптимізації сонячного елемента для досягнення найкращої продуктивності. Чисельне моделювання для опису фотоелементних тонкошарових пристроїв є зручним інструментом для кращого розуміння основних факторів, що обмежують електричні параметри сонячних елементів, і для підвищення їх продуктивності. У цій оглядовій статті ми зосередилися на останніх досягненнях у моделюванні та оптимізації PSC за допомогою SCAPS-1D з акцентом на товщину поглиначка та електронно-транспортного середовища (ЕТМ).

Ключові слова: перовскітові сонячні батареї, поглинач, електронне транспортне середовище, SCAPS